

The International Society of Precision Agriculture presents the  
**16<sup>th</sup> International Conference on  
Precision Agriculture**  
21–24 July 2024 | Manhattan, Kansas USA



## **In-Season Diagnosis of Corn Nitrogen and Water Status Using UAV Multispectral and Thermal Remote Sensing**

Ayoub Kechchour<sup>1</sup>, Yuxin Miao<sup>1</sup>, Vasudha Sharma<sup>1</sup>, Andrea Flores<sup>1</sup>, Lorena Lacerda<sup>2</sup>, Katsutoshi Mizuta<sup>1</sup>, Junjun Lu<sup>1</sup>, Yanbo Huang<sup>3</sup>

<sup>1</sup> Precision Agriculture Center, University of Minnesota, St. Paul, MN 55108, USA

<sup>2</sup> Department of Crop and Soil Sciences, University of Georgia, Athens, GA 30602, USA

<sup>3</sup> Genetics and Sustainable Agriculture Research Unit, USDA-ARS, Mississippi State, MS USA

**A paper from the Proceedings of the  
16<sup>th</sup> International Conference on Precision Agriculture  
21-24 July 2024  
Manhattan, Kansas, United States**

### **Abstract.**

*For irrigated corn fields, how to optimize nitrogen (N) and irrigation simultaneously is a great challenge. A promising strategy is to use remote sensing to diagnose corn N and water status during the growing season, which can then be used to guide in-season variable rate N application and irrigation management. The objective of this study was to evaluate the effectiveness of UAV multispectral and thermal remote sensing in simultaneous diagnosis of corn N and water status. Two field experiments were conducted in Becker and Westport, Minnesota in 2021, 2022 and 2023 using a split plot design with four replications, involving four irrigation treatments (100% FI (full irrigation), 75% FI, 50% FI, and 0% FI (rainfed)) for 2021 and 2022, and FI (125%), 100% FI, 65% FI, and rainfed (0% FI) for 2023 as main plots and six N rate treatments (0, 78, 157, 235, 314, and 392 kg ha<sup>-1</sup>) as subplots. Soil moisture data from four different depths were collected once a week in each field. A UAV (unmanned aerial vehicle) remote sensing system with MicaSense Altum camera was used to simultaneously collect multispectral and thermal images at different growth stages across the growing season. Plant samples were collected at V8, R1 and R6 to analyze aboveground biomass, plant N concentration and plant N uptake and N nutrition index (NNI) was calculated as a reliable indicator of crop N status. With UAV image data, different vegetation indices were calculated and related to crop N status indicators and soil moisture conditions to identify the indices sensitive to corn N and water status. Machine learning models were developed using remote sensing data, weather, and management information to*

*predict corn N and water status. Using agronomic data collected from these experiments, field plots were labelled as “Water Stress”, “Nitrogen Stress”, “No Stress” or “Water and Nitrogen Stress”. Analysis indicated that the combination of the Crop Water Stress Index (CWSI) and Reference Evapotranspiration ( $ET_0$ ) contributed the most to detecting water stress. For nitrogen stress, the combination of the Normalized Difference Red Edge (NDRE) and the Normalized Difference Vegetation Index (NDVI) proved effective. For no stress and combined water-nitrogen stress, the optimal combinations were NDRE with CWSI and  $ET_0$  with NDRE, respectively. The best model (XGBoost) achieved an accuracy, recall, and F1-score of 0.61-0.62.*

**Keywords.**

*Nitrogen status, Water stress, Multispectral remote sensing, Thermal remote sensing, Precision nitrogen management, Precision irrigation.*

## **Introduction**

The world population has been projected to around 8.5 billion in 2030 and 9.7 billion in 2050 (United Nation., 2022). As a result, producing 70 percent more food is mandatory to attain food security (FAO, 2009). However, this increase should be accompanied by sustainable enhancement and efficient management of natural resources to meet the UN's Sustainable Development Goals (SDGs) (Kroll et al., 2019). This boost in production generally carries an environmental cost and ecosystem disservices, including biodiversity loss, sedimentation of waterways, nutrient pollution, and greenhouse gas emissions. (Dale & Polasky, 2007; Zhang et al., 2007)

To direct agriculture towards a sustainable pathway, there is a strong demand for using precision agriculture in general and variable rate application technology in particular, which allows monitoring of the food supply chain and manage both the quantity and quality of agricultural inputs and outputs, applying the proper treatment in the right place at the right time (Barrett, 2010), optimizing the use of available resources to increase the profitability and sustainability of agricultural operations and reduce environmental cost of the management practices (Gebbers & Adamchuk, 2010).

Vegetation indices are a very straightforward but robust method to extract the green plant quantity signal and information from complex canopy spectra. Thus, they provide a guide to understanding spatial-temporal variations of crop nitrogen (N) status, allowing the adaptation of N application to crop N requirements (Quemada et al., 2014). Before attaining full canopy cover, soil background effect on reflectance is more visible, making it difficult to distinguish between soil and plant spectral components. Separating components at early growth stages is crucial, as the N prescription plan is made at early stages (Basso et al., 2009)).on the path to minimize this problem, Canopy Chlorophyll Content Index (CCCI) was developed, which can adapt to mixed soil/plant pixel by plotting chlorophyll index and biomass related index in a two-dimensional space (Clarke et al., 2001). In addition, water stress reduces the ability of VI to estimate plant traits (Kusnierek & Korsath, 2015; Schepers et al., 1996)

Foliar temperature is inversely influenced by the transpiration. Leaf temperature has long been used as proxy for water stress (Tanner, 1963). The leaf and air temperature difference has been widely used to detect plant water stress (Idso et al., 1977). However, to overcome the limitations of other environmental factors influencing plant water, the Crop Water Stress Index (CWSI) was developed (Idso, 1982).

The aim of the study was to investigate the potential of using machine learning classification with vegetation indices derived from UAV images with soil and weather variables to separate crop N and water stress.

# Material and Methods

## Study Design

The study was carried out over three years (2021-2023) in Becker and Westport, MN and employed a split-plot design (Figure 1). The main plots consisted of four irrigation treatments: full irrigation (FI: 100%), 75% FI, 50% FI, and rainfed (0% FI) for 2021 and 2022, and FI (125%), 100% FI, 65% FI, and rainfed (0% FI) for 2023. These treatments were coded as I1, I2, I3, and I4, respectively. Subplots included six N rate treatments: 0, 78, 157, 235, 314, and 392 kg/ha. These treatments were coded as N1, N2, N3, N4, N5 and N6, respectively. Each treatment combination was replicated four times across the the two fields to assess the N and water status of the corn crops.

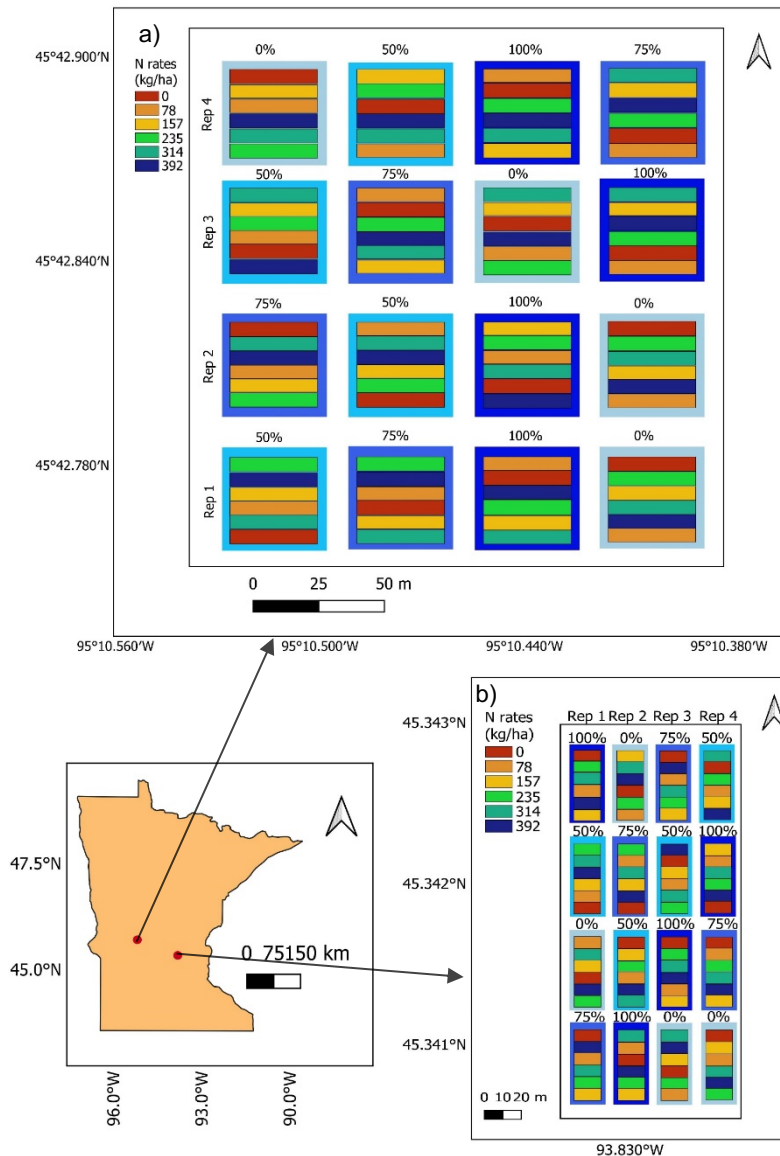


Figure 1: Experimental field locations in the state of Minnesota and plot layouts in (a) Westport and (b) Becker.

Plant sampling data were collected from entire length of two middle rows in each plot for V8, R1 and R6. The information on management practices and sensing date is summarized in table 1

Table 1 : Information on the details of the experiments conducted in 2021, 2022 and 2023

Year	Location	Growth Stage	Planting date	Side-dress date	Harvest date	Sampling Date	Sensing Date
2021	Westport	V8				June 29	Aug 6
		R1	May 18	June 28	Nov 3	July 29	Aug 25
		R6				Oct 5	
	Becker	V8				June 25	Aug 16
		R1	May 7	June 25	Oct 22	July 23	Aug 25
		R6				Sep 27	Aug 31
2022	Westport	V8				July 6	Aug 10
		R1	June 23	July 6	Nov 18	Aug 3	Aug 31
		R6				Sep 5	Sep 12
	Becker	V8				June 28	July13 - July 27
		R1	May 16	June 28	Sep 31	July 27	Aug 10 - Aug 23
		R6				Sep 6	Aug 31 – Sep 27
2023	Westport	V8				June 22	June 22 – July 7
		R1	May 11	June 22	Oct 17	July 31	July 12 - Aug 29
		R6				Sep 28	
	Becker	V8				June 23	June 20 - July 6
		R1	May 4	June 15	Oct 22	July 19	July 13 - July 25
		R6				Sep 7	Aug 8 - Aug 29

## Crop N Status Diagnosis

Six samples from rows 4-5 of whole plant per plot were collected three times at V8, R1 and R6 stages in each year. The first sampling coincided with the side-dress application. Two types of samples were taken: aerial biomass and total plant N from six plants.

To determine corn N status, the N nutrition index (NNI) was calculate by using critical dilution curve for corn proposed by (Plénet & Lemaire, 1999), linking corn N dilution with dry matter and leaf area expansion. It can be calculated using the following equation:

$$NNI = \frac{\%N_a}{\%N_c} \quad (1)$$

Where  $\%N_c = 3.6 \times biomass^{-0.34}$  is the minimum N concentration needed to produce the maximum growth. Nevertheless, the NNI is not a real-time assessment method. It necessitates destructive sampling, subsequent quantification of plant N concentration, and measurement of aerial biomass. Despite its accuracy, this process is labor-intensive and time-consuming, rendering it impractical for real-time field applications and large-scale agricultural operations(Cao et al., 2012; Li et al., 2022; Miao et al., 2009; Peng et al., 2010; Prost & Jeuffroy, 2007). Additionally, under water stress conditions, the thresholds of the NNI that delineate under-fertilization and over-fertilization lose their validity. This is due to the varying degrees of stress

impacting the plant's physiological responses, altering the accuracy of NNI thresholds.(Gonzalez-Dugo et al., 2010).

### Spectral and thermal measurements

The Canopy Chlorophyll Content Index (CCCI) is a widely recognized planar domain index. It utilizes structural vegetation indices (VI) as proxies for crop biomass, and chlorophyll related VI for crop N concentration, as outlined by Barnes et al.(2000) and Fitzgerald et al.( 2010). In this study, CCCI for each plot was calculated using a two-dimensional framework where NDVI values were plotted on the X-axis and NDRE on the Y-axis. The proximity of each data point to the top and bottom lines, which represent the range of data starting from the coordinate origin, determines the CCCI value. Plots with adequate N tend to align closer to the upper line, whereas N-deficient plots are nearer to the lower line. As N status considered as secondary variable, which cannot be directly related to remotely sensed observations (Weiss et al., 2020), the most VIs developed use other biophysical variables as chlorophyll content or biomass without taking in consideration other limiting factors that may influence the N dilution curve(Mistele & Schmidhalter, 2008). Furthermore, the optimal N content is dependent on biomass, which can be significantly affected by drought conditions (Lemaire et al., 2008; Pancorbo et al., 2021; Sadras & Lemaire, 2014), making the estimation of crop traits through vegetation indices inefficient when crops are suffering from water stress.

Under field conditions, crops have varying N fertilization requirements due to differences in soil conditions, landscape conditions, and water stress levels (Ma et al., 2015). To address this issue, incorporating a water stress indicator appears essential for gaining more accurate insights into N requirements.

### Crop water stress detection

Thermal infrared imaging is a highly effective method for assessing water status and optimizing irrigation. the study incorporated temperature-based vegetation indices like the canopy-air temperature difference ( $T_c - T_a$ ) (Idso et al., 1977), and CWSI (Idso, 1982; Jackson et al., 1977). CWSI can be calculated by using (Eq. 2):

$$CWSI_i = \frac{(T_c - T_a) - (T_c - T_a)_{LL}}{(T_c - T_a)_{UL} - (T_c - T_a)_{LL}} \quad (2)$$

Where  $(T_c - T_a)_{LL}$  is the lower threshold indicating a well-watered condition;  $(T_c - T_a)_{UL}$  is the upper limit representing the stressed condition. The two CWSI models differ in the methods used to calculate the upper and lower limits.

The Theoretical CWSI ( $CWSI_T$ ) is using the energy balance equation and the Penman–Monteith equation (Jackson et al., 1981). Where  $(T_c - T_a)_{UL}$  and  $(T_c - T_a)_{LL}$  can be calculated by:

$$(T_c - T_a)_{UL} = \frac{r_a(R_n - G)}{pc_p} \quad (3)$$

$$(T_c - T_a)_{LL} = \frac{r_a(R_n - G)}{pc_p} \times \frac{\gamma}{\gamma + \Delta} - \frac{VPD}{\gamma + \Delta} \quad (4)$$

where  $r_a$  represents the aerodynamic resistance (s/m),  $R_n$  denotes the net solar radiation ( $W/m^2$ ),  $G$  is the soil heat flux ( $W/m^2$ ),  $c_p$  signifies the heat capacity of air ( $J/(kg \cdot K)$ ),  $\gamma$  is the psychrometric constant (Pa/K),  $\Delta$  is the slope of the saturated vapor pressure curve relative to temperature (Pa/K), and VPD refers to the vapor pressure deficit (Pa).

The empirical CWSI ( $CWSI_E$ ) was first presented by (Idso, 1982), where a  $T_c - T_a$  of a well-watered crops follows a linear relationship with VPD, following this principle  $(T_c - T_a)_{LL}$  can be calculated as is in Eq. 5:

$$(T_c - T_a)_{LL} = a \times VPD + b \quad (5)$$

Using data from three years and 982 observations, the coefficient and intercept were determined as follows:  $a = -1.30$  and  $b = 3.60$ .

Considering  $(T_c - T_a)_{UL}$ , it can be calculated by (Eq. 6) where  $T_c$  is from a stressed crop.(Katimbo et al., 2022):

$$(T_c - T_a)_{LL} = \max(T_c - T_a) \quad (6)$$

To ensure the accuracy and consistency of the Crop Water Stress Index (CWSI) in our model, we normalized the empirical CWSI ( $CWSI_E$ ) using a min-max scaler(Patro & Sahu, 2015). This normalization process scales the  $CWSI_E$  values to a range between 0 and 1, making them comparable and reducing the potential influence of outliers.

$$CWSI_{normalized} = \frac{CWSI_E - \min(CWSI_E)}{\max(CWSI_E) - \min(CWSI_E)} \quad (7)$$

### Development and Evaluation of the Machine learning model :

Expert knowledge and agronomic data were utilized to label the plots based on stress categories: N Stress, Water Stress, Water and N Stress, and No Stress. This classification follows the criterion that more than a ten percent reduction in relative yield is considered a deficiency zone for both water and N consumption.(Fowler, 2003; Heins & Yelanich, 2013; Isaac & Kimaro, 2011; Memon et al., 2005).

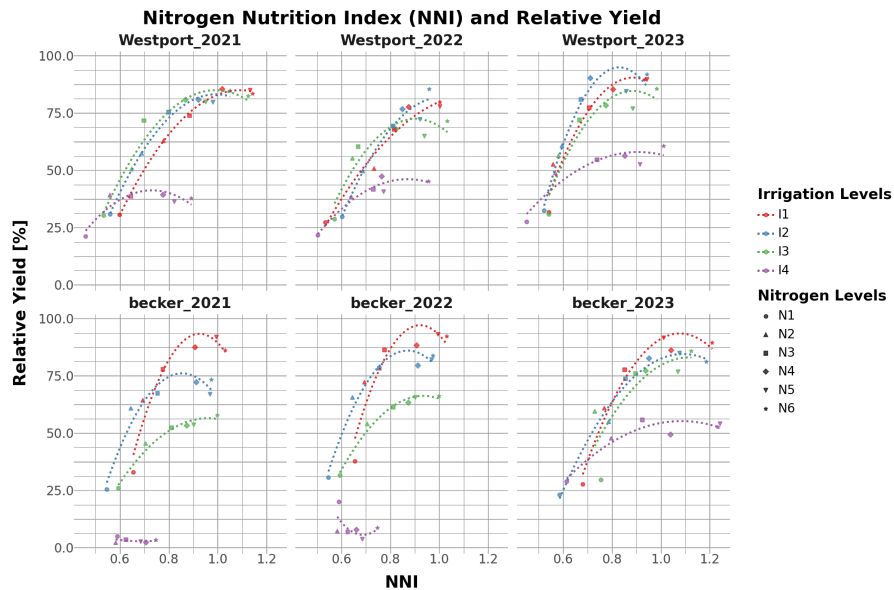


Figure 2: NNI relationship with relative yield

In our study, we identified an imbalance in the stress category data, with certain categories being underrepresented. This imbalance could significantly impact the performance and accuracy of our machine learning models.

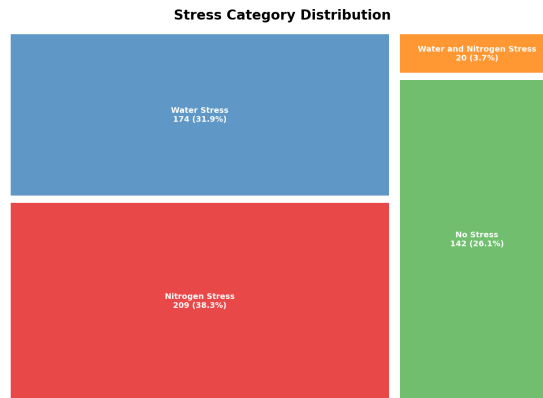


Figure 3: Stress Category distribution.

To address this issue, we employed the Synthetic Minority Over-sampling Technique (SMOTE) to balance the dataset (Chawla et al., 2002). SMOTE generated synthetic samples for the underrepresented categories, ensuring each stress category was adequately represented. This step was crucial to avoid biased predictions and to enhance the reliability and robustness of our machine learning models.

Our research was primarily focused on the V8 growth stage of corn. This stage is critical for early season stress condition identification, which is necessary for prompt and informed decisions about irrigation schedules and side-dress N applications. By concentrating on V8, we can precisely detect water stress as well as N stress, enabling us to make improvements to management procedures. This strategy supports sustainable agriculture practices by enhancing crop health, optimizing resource use, and increasing yield potential.

We used the machine learning algorithm XGBoost (Chen & Guestrin, 2016) to categorize the stress conditions using cross validation (Browne, 2000). Furthermore, we used explainable artificial intelligence (XAI) with SHAP (SHapley Additive exPlanations) (Lundberg & Lee, 2017), which gave us insights into the role of each feature in the model. Robust and transparent stress detection was guaranteed by this mix of advanced classification and interpretability algorithms, which will help with accurate and efficient in-season management decisions.

## Results

This combination of advanced classification and interpretability techniques ensured robust and transparent stress detection, aiding in precise and effective in-season management decisions.

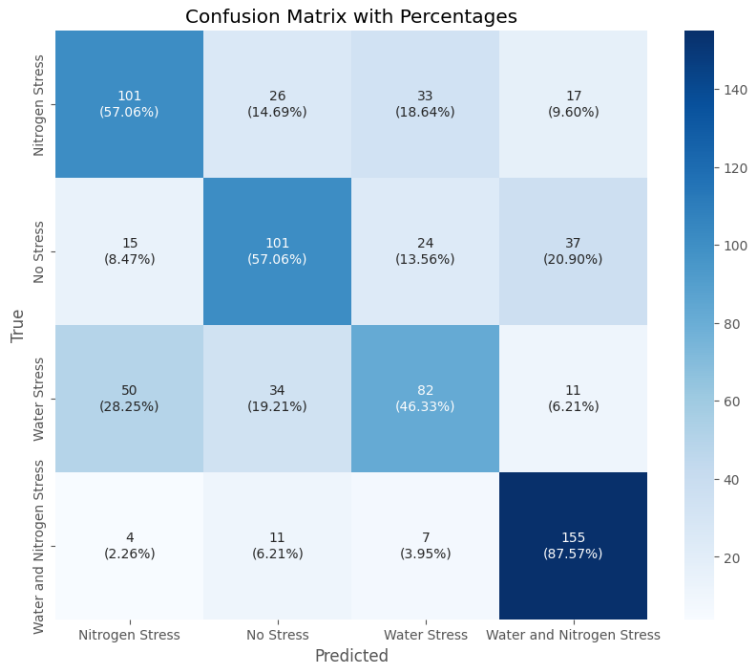
Cross-validation was used to assess the model's performance, yielding the following metrics.

Table 2: Performance Metrics of the XGBoost Model for Different Stress Conditions

Stress Condition	precision	recall	f1-score
Nitrogen Stress	0.59	0.57	0.58
No Stress	0.59	0.57	0.58
Water Stress	0.56	0.46	0.51
Water and Nitrogen Stress	0.7	0.88	0.78
<b>accuracy</b>	0.62	0.62	0.62
<b>macro avg</b>	0.61	0.62	0.61
<b>weighted avg</b>	0.61	0.62	0.61

The results indicate that the model achieved a cross-validation accuracy of 0.62, with varying performance across different stress conditions. Notably, the model performed best in detecting combined water and N stress, achieving a precision of 0.70, recall of 0.88, and an F1-score of 0.78. However, it is important to note that the high performance in this category may be due to overfitting, because of applying the SMOTE to balance the dataset. The use of SHAP provided valuable insights into the feature contributions, enhancing the interpretability of the model's predictions.

The confusion matrix below further illustrates the model's performance, showing the distribution of predicted versus actual stress conditions:



**Figure 4: Confusion Matrix with percentages**

To further illustrate the contribution of features to the predictions for various stress conditions, unique SHAP force charts were created. These charts illustrate the influence of each attribute on the likelihood that the model will forecast a particular stress condition:



Figure 5: SHAP Force Plots for different stress conditions

The SHAP force plots offer an in-depth comprehension of the ways in which various variables influence the stress conditions that are predicted. The arrows show the direction and amount of each feature's contribution, and the x-axis shows the model's likelihood of predicting a certain stress situation.

- **Nitrogen Stress:** Tc-Ta, CWSI\_T, and ET<sub>0</sub> are the primary contributors (highlighted in red) that raise the likelihood of N stress. On the other hand, the blue-highlighted NDVI and NDRE reduce the likelihood of N stress.
- **Water Stress:** The chance of water stress is considerably increased by features like CWSI\_T and ET<sub>0</sub>, which are indicated in red. Conversely, the probability of water stress is reduced by solar radiation and NDRE, which are indicated in blue.
- **No Stress:** The red features that raise the likelihood of no stress are accumulated GDD, ET<sub>0</sub>, and NDRE. The chance of there being no stress is decreased by blue characteristics like (T<sub>c</sub> - T<sub>a</sub>) and CWSI\_normalized.
- **Water and N Stress:** The probability of both water and N stress combined is increased by solar radiation and CWSI\_normalized, which are indicated in red. On the other hand, the blue-highlighted ET<sub>0</sub>, CWSI\_T, Tc-Ta, and NDVI reduce the likelihood of this combined stress situation.

Developing a threshold using CWSI to start irrigation is crucial for effective water management. The following figure focuses on the impact of the normalized CWSI (CWSI\_normalized) on water stress prediction:

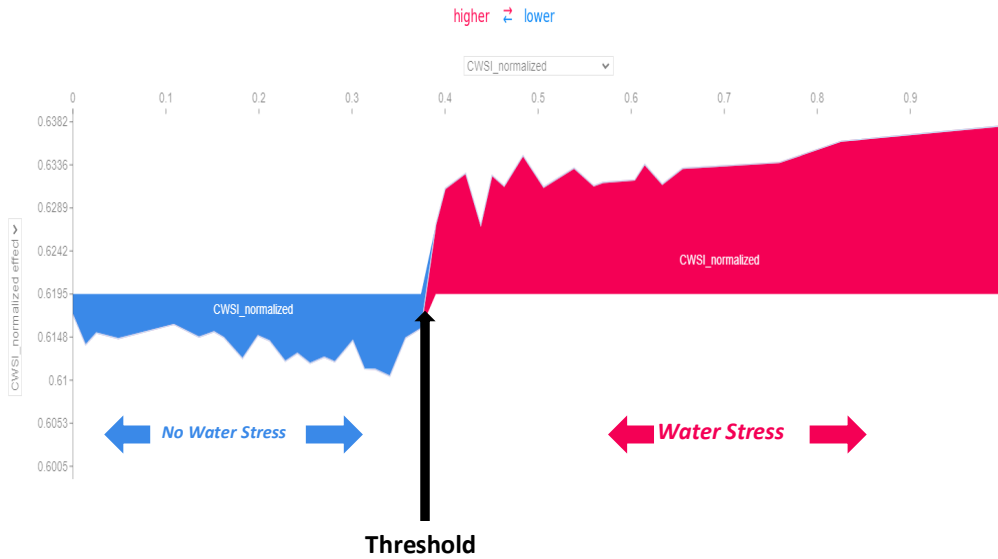


Figure 6: Combined SHAP CWSI Force Plot for water stress

In this combined SHAP force plot, the x-axis represents the model's ability to predicting water stress, with higher values (red) indicating increased likelihood of water stress and lower values (blue) corresponding to no water stress. The illustration above emphasizes how important CWSI\_normalized is in identifying the circumstances behind water stress. The best time to start irrigation can be found by setting a threshold for CWSI\_normalized, which will increase crop health and water use efficiency.

Similarly, to develop a threshold using CCCI to detect N stress, the following figure focuses on the impact of the CCCI index on N stress prediction:

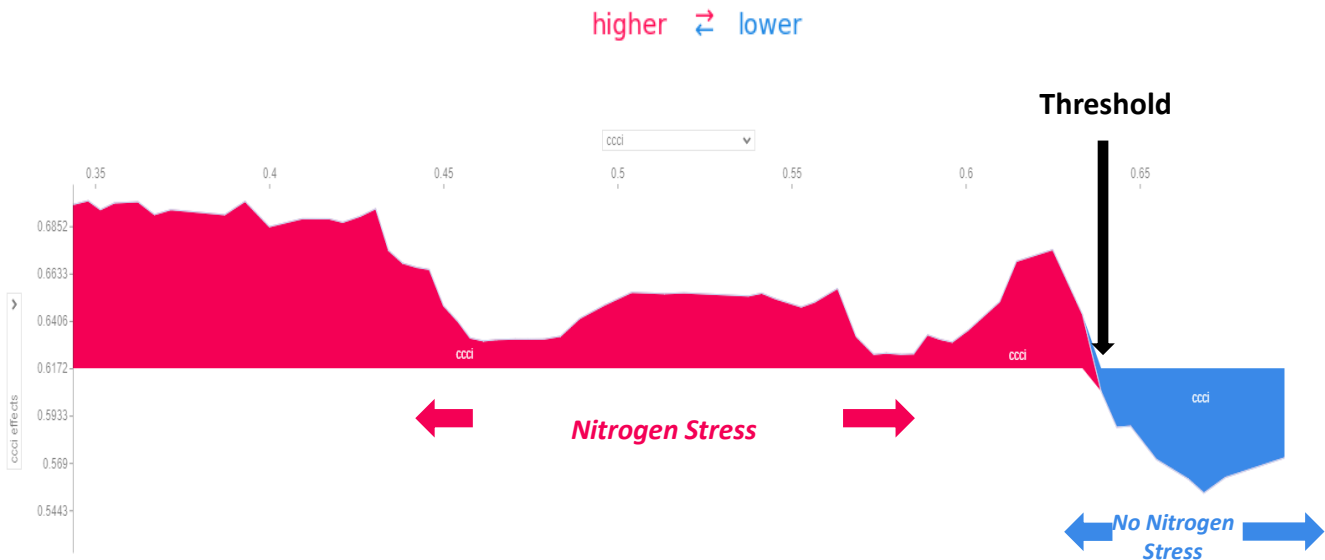


Figure 7: Combined SHAP CCCI Force Plot for N stress

## Discussion and Conclusion

The ability of UAV multispectral and thermal remote sensing to identify water stress and N deficiency in corn throughout the growing season was effectively illustrated by this study. Using machine learning models, specifically XGBoost, and the interpretability of SHAP, we achieved a remarkable degree of accuracy and transparency in the classification of different stress conditions. The integration of these cutting-edge methods enabled solid and accurate in-season management choices, which are essential for optimal resource utilization in precision farming.

To correctly identify and address corn N and water stress, the study emphasizes the need of combining multispectral and thermal remote sensing data with cutting-edge machine learning algorithms. We can optimize N fertilization and irrigation techniques by determining thresholds for important indices like CWSI<sub>normalized</sub> and NDRE and by comprehensively considering the contributions of specific features.

The findings also highlight the necessity of connecting stress detection to practical management techniques. This entails figuring out the best time and quantity for fertilizer and watering in addition to detecting the kind of stress. Precise suggestions will be made possible by integrating CWSI with data on water balance (WB) and evapotranspiration, as well as connecting NDRE with rates of N application. This will guarantee effective resource utilization and sustainable farming practices.

In conclusion, explainable AI, machine learning, and UAV-based remote sensing offer a potent tool for precision agriculture. This strategy improves our capacity to dynamically monitor and control crop health, which eventually raises the possibility of increasing yield and resource efficiency. Further studies should concentrate on enhancing these models and investigating their use in diverse crop systems and environments in order to improve their potential for use in precision agriculture.

## Acknowledgements

This project was funded by the Agricultural Fertilized Research and Education Council (AFREC) Data collection was assisted by Dr. Vasudha Sharma's lab members, staff at the Rosholt Research Farm and student workers from the UMN's Crop Research.

## References

- Barnes, E., Clarke, T. R., Richards, S. E., Colaizzi, P., Haberland, J., Kostrzewski, M., Waller, P., Choi, C., Riley, E., & Thompson, T. L. (2000). *Coincident detection of crop water stress, nitrogen status, and canopy density using ground based multispectral data*.
- Basso, B., Cammarano, D., Grace, P. R., Cafiero, G., Sartori, L., Pisante, M., Landi, G., Franchi, S. D., & Basso, F. (2009). Criteria for Selecting Optimal Nitrogen Fertilizer Rates for Precision Agriculture. *Italian Journal of Agronomy*, 4(4), Article 4. <https://doi.org/10.4081/ija.2009.4.147>
- Browne, M. W. (2000). Cross-validation methods. *Journal of Mathematical Psychology*, 44(1), 108–132.
- Cao, Q., Cui, Z., Chen, X., Khosla, R., Dao, T. H., & Miao, Y. (2012). Quantifying spatial variability of indigenous nitrogen supply for precision nitrogen management in small scale farming. *Precision Agriculture*, 13(1), 45–61. <https://doi.org/10.1007/s11119-011-9244-3>
- Chawla, N. V., Bowyer, K. W., Hall, L. O., & Kegelmeyer, W. P. (2002). SMOTE: Synthetic Minority Over-sampling Technique. *Journal of Artificial Intelligence Research*, 16, 321–357. <https://doi.org/10.1613/jair.953>

- Clarke, T. R., Moran, M. S., Barnes, E. M., Pinter, P. J., & Qi, J. (2001). Planar domain indices: A method for measuring a quality of a single component in two-component pixels. *IGARSS 2001. Scanning the Present and Resolving the Future. Proceedings. IEEE 2001 International Geoscience and Remote Sensing Symposium (Cat. No.01CH37217)*, 3, 1279–1281 vol.3. <https://doi.org/10.1109/IGARSS.2001.976818>
- Dale, V. H., & Polasky, S. (2007). Measures of the effects of agricultural practices on ecosystem services. *Ecological Economics*, 64(2), 286–296. <https://doi.org/10.1016/j.ecolecon.2007.05.009>
- Fitzgerald, G., Rodriguez, D., & O'Leary, G. (2010). Measuring and predicting canopy nitrogen nutrition in wheat using a spectral index—The canopy chlorophyll content index (CCCI). *Field Crops Research*, 116(3), 318–324. <https://doi.org/10.1016/j.fcr.2010.01.010>
- Fowler, D. B. (2003). Crop Nitrogen Demand and Grain Protein Concentration of Spring and Winter Wheat. *Agronomy Journal*, 95(2), 260–265. <https://doi.org/10.2134/agronj2003.2600>
- Gebbers, R., & Adamchuk, V. I. (2010). Precision agriculture and food security. *Science (New York, N.Y.)*, 327(5967), 828–831. <https://doi.org/10.1126/science.1183899>
- Gonzalez-Dugo, V., Durand, J.-L., & Gastal, F. (2010). Water deficit and nitrogen nutrition of crops. A review. *Agronomy for Sustainable Development*, 30(3), Article 3. <https://doi.org/10.1051/agro/2009059>
- Heins, R. D., & Yelanich, M. (2013). *Fertilization regimes exceed nutritional requirements of greenhouse crops. 1(PART 1)*. Scopus. <https://doi.org/10.3182/20130327-3-jp-3017.00004>
- Idso, S. B. (1982). Non-water-stressed baselines: A key to measuring and interpreting plant water stress. *Agricultural Meteorology*, 27(1), 59–70. [https://doi.org/10.1016/0002-1571\(82\)90020-6](https://doi.org/10.1016/0002-1571(82)90020-6)
- Idso, S. B., Jackson, R. D., & Reginato, R. J. (1977). Remote-Sensing of Crop Yields. *Science*, 196(4285), 19–25. <https://doi.org/10.1126/science.196.4285.19>
- Isaac, M., & Kimaro, A. (2011). Diagnosis of Nutrient Imbalances with Vector Analysis in Agroforestry Systems. *Journal of Environmental Quality*, 40, 860–866. <https://doi.org/10.2134/jeq2010.0144>
- Jackson, R. D., Idso, S. B., Reginato, R. J., & Pinter Jr., P. J. (1981). Canopy temperature as a crop water stress indicator. *Water Resources Research*, 17(4), 1133–1138. <https://doi.org/10.1029/WR017i004p01133>
- Jackson, R. D., Reginato, R. J., & Idso, S. B. (1977). Wheat canopy temperature: A practical tool for evaluating water requirements. *Water Resources Research*, 13(3), 651–656. <https://doi.org/10.1029/WR013i003p00651>
- Katimbo, A., Rudnick, D. R., DeJonge, K. C., Lo, T. H., Qiao, X., Franz, T. E., Nakabuye, H. N., & Duan, J. (2022). Crop water stress index computation approaches and their sensitivity to soil water dynamics. *Agricultural Water Management*, 266. Scopus. <https://doi.org/10.1016/j.agwat.2022.107575>
- Kroll, C., Warchold, A., & Pradhan, P. (2019). Sustainable Development Goals (SDGs): Are we successful in turning trade-offs into synergies? *Palgrave Communications*, 5(1), 1–11. <https://doi.org/10.1057/s41599-019-0335-5>
- Kusnierek, K., & Korsaeath, A. (2015). Simultaneous identification of spring wheat nitrogen and water status using visible and near infrared spectra and Powered Partial Least Squares Regression. *Computers and Electronics in Agriculture*, 117, 200–213. <https://doi.org/10.1016/j.compag.2015.08.001>
- Lemaire, G., Jeuffroy, M.-H., & Gastal, F. (2008). Diagnosis tool for plant and crop N status in vegetative stage. Theory and practices for crop N management. *European Journal of Agronomy*, 28(4), 614–624. Scopus. <https://doi.org/10.1016/j.eja.2008.01.005>
- Li, X., Ata-Ul-Karim, S. T., Li, Y., Yuan, F., Miao, Y., Yoichiro, K., Cheng, T., Tang, L., Tian, X., Liu, X., Tian, Y., Zhu, Y., Cao, W., & Cao, Q. (2022). Advances in the estimations and applications of critical nitrogen dilution curve and nitrogen nutrition index of major cereal crops. A review. *Computers and Electronics in Agriculture*, 197, 106998.

<https://doi.org/10.1016/j.compag.2022.106998>

- Lundberg, S. M., & Lee, S.-I. (2017). *A unified approach to interpreting model predictions*. 2017-December, 4766–4775. Scopus.
- Memon, N., Memon, K., & Shah, Z. (2005). Plant Analysis as a diagnostic tool for evaluating nutritional requirements of bananas. *International Journal of Agriculture and Biology*, 7, 824–831.
- Miao, Y., Mulla, D. J., Randall, G. W., Vetsch, J. A., & Vintila, R. (2009). Combining chlorophyll meter readings and high spatial resolution remote sensing images for in-season site-specific nitrogen management of corn. *Precision Agriculture*, 10(1), 45–62. <https://doi.org/10.1007/s11119-008-9091-z>
- Mistele, B., & Schmidhalter, U. (2008). Estimating the nitrogen nutrition index using spectral canopy reflectance measurements. *European Journal of Agronomy*, 29(4), 184–190. Scopus. <https://doi.org/10.1016/j.eja.2008.05.007>
- Pancorbo, J. L., Camino, C., Alonso-Ayuso, M., Raya-Sereno, M. D., Gonzalez-Fernandez, I., Gabriel, J. L., Zarco-Tejada, P. J., & Quemada, M. (2021). Simultaneous assessment of nitrogen and water status in winter wheat using hyperspectral and thermal sensors. *European Journal of Agronomy*, 127, 126287. <https://doi.org/10.1016/j.eja.2021.126287>
- Patro, S. G. K., & Sahu, K. K. (2015). *Normalization: A Preprocessing Stage* (arXiv:1503.06462). arXiv. <https://doi.org/10.48550/arXiv.1503.06462>
- Peng, S., Buresh, R. J., Huang, J., Zhong, X., Zou, Y., Yang, J., Wang, G., Liu, Y., Hu, R., Tang, Q., Cui, K., Zhang, F., & Dobermann, A. (2010). Improving nitrogen fertilization in rice by sitespecific N management. A review. *Agronomy for Sustainable Development*, 30(3), 649–656. <https://doi.org/10.1051/agro/2010002>
- Plénet, D., & Lemaire, G. (1999). Relationships between dynamics of nitrogen uptake and dry matter accumulation in maize crops. Determination of critical N concentration. *Plant and Soil*, 216(1), 65–82. <https://doi.org/10.1023/A:1004783431055>
- Prost, L., & Jeuffroy, M.-H. (2007). Replacing the nitrogen nutrition index by the chlorophyll meter to assess wheat N status. *Agronomy for Sustainable Development*, 27(4), 321–330. <https://doi.org/10.1051/agro:2007032>
- Quemada, M., Gabriel, J. L., & Zarco-Tejada, P. (2014). Airborne Hyperspectral Images and Ground-Level Optical Sensors As Assessment Tools for Maize Nitrogen Fertilization. *Remote Sensing*, 6(4), Article 4. <https://doi.org/10.3390/rs6042940>
- Sadras, V. O., & Lemaire, G. (2014). Quantifying crop nitrogen status for comparisons of agronomic practices and genotypes. *Field Crops Research*, 164(1), 54–64. Scopus. <https://doi.org/10.1016/j.fcr.2014.05.006>
- Schepers, J. S., Blackmer, T. M., Wilhelm, W. W., & Resende, M. (1996). Transmittance and Reflectance Measurements of Corn Leaves from Plants with Different Nitrogen and Water Supply. *Journal of Plant Physiology*, 148(5), 523–529. [https://doi.org/10.1016/S0176-1617\(96\)80071-X](https://doi.org/10.1016/S0176-1617(96)80071-X)
- Tanner, C. B. (1963). Plant Temperatures<sup>1</sup>. *Agronomy Journal*, 55(2), 210–211. <https://doi.org/10.2134/agronj1963.00021962005500020043x>
- Weiss, M., Jacob, F., & Duveiller, G. (2020). Remote sensing for agricultural applications: A meta-review. *Remote Sensing of Environment*, 236. Scopus. <https://doi.org/10.1016/j.rse.2019.111402>
- Zhang, W., Ricketts, T. H., Kremen, C., Carney, K., & Swinton, S. M. (2007). Ecosystem services and dis-services to agriculture. *Ecological Economics*, 64(2), 253–260. <https://doi.org/10.1016/j.ecolecon.2007.02.024>